

Electronic Supplementary Information

Self-inverted Reciprocation of an Oil Droplet on a Surfactant Solution

Yusuke Satoh^a, Yoshimi Sogabe^b, Katsuhiko Kayahara^b, Shinpei Tanaka^c, Masaharu Nagayama^{*a}, Satoshi Nakata^{**b}

^a Graduate School of Science, Hokkaido University, N10W8, Kita-Ward, Sapporo, 060-0810, Japan

^b Graduate School of Science, Hiroshima University, 1-3-1 Kagamiyama, Higashi-Hiroshima 739-8526, Japan

^c Graduate School of Integrated Arts and Sciences, Hiroshima University, 1-7-1 Kagamiyama, Higashi-Hiroshima 739-8521, Japan

^d Research Institute for Electronic Science, Hokkaido University, N20W10, Kita-Ward, Sapporo, 001-0020, Japan

*, ** To whom correspondence should be addressed.

** Tel.: +81-11-706-3357, E-mail: nagayama@es.hokudai.ac.jp

* Tel.: +81-82-424-7409, E-mail: nakatas@hiroshima-u.ac.jp

1. Movies for experimental results in Figure 1

Movie S1. Movie of reciprocating motion in Fig. 1a (real time)

Movie S2. Movie of reciprocating motion in Fig. 1b (real time)

2. Time-course of reciprocating motion in the long-term observation

Figure S1 shows the time-course of the location of a BS droplet on the longitudinal axis of the rectangular glass vessel (300 mm (length) \times 15 mm (width) \times 10 mm (height)), x , at $C_{\text{SDS-w}} =$ (a) 20 and (b) 60 mM in the long-term observation. Reciprocating motion maintained for a few hours, and then finally stopped.

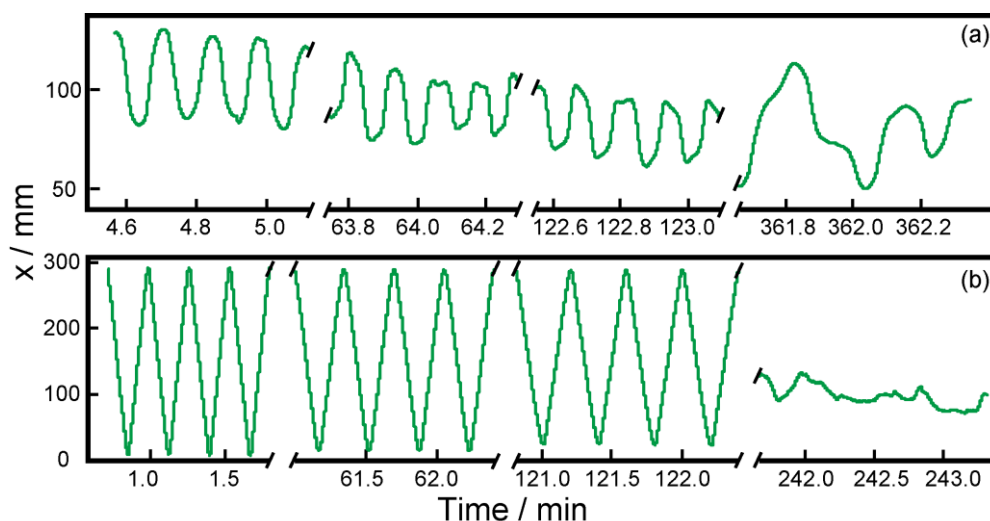


Figure S1. Time-course of the location of a BS droplet on the longitudinal axis of the chamber, x , at different concentrations of SDS in the water phase ($C_{\text{SDS-w}} =$ (a) 20 and (b) 60 mM). $x = 0$ corresponds to the location of one edge of the water chamber.

3. Reciprocating motion with a small amplitude in an annular water chamber

Figure S2 shows snapshots of reciprocating motion with a small amplitude at $C_{\text{SDS-w}} = 20 \text{ mM}$ when an annular glass chamber (inner diameter: 90 mm, width of the chamber: 18 mm) was used to confirm the effect of the boundary of chamber.

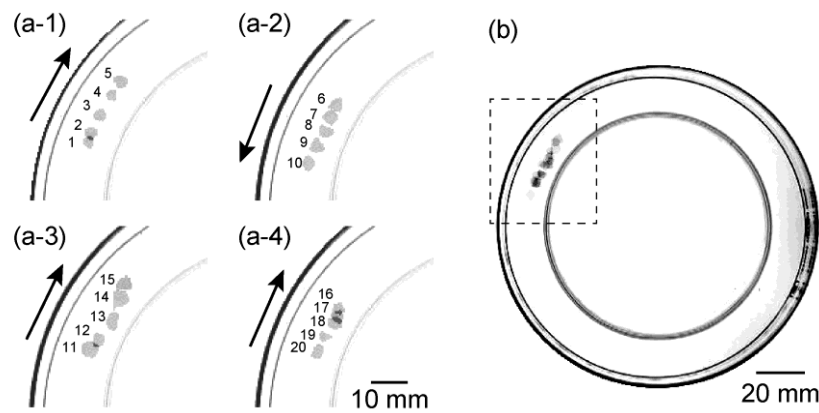


Figure S2. Snapshots of (a) a BS droplet (time interval: 0.2 s) and (b) annular water chamber (top view). Observation time was (a-1) 120.7 - 121.5 s (No.1-5), (a-2) 124.0 - 124.8 s (No.6-10), (a-3) 128.0 - 128.8 s (No.11-15), and (a-4) 131.0 - 131.8 s (No.16-20). The dotted square in (b) corresponds to the observation region in (a).

4. Experimental results on the simultaneous measurement of speed and ellipticity of a BS droplet

Figure S3 shows the experimental results on the simultaneous measurement of speed (solid line) and ellipticity, l_x/l_y , (dotted line) of a BS droplet which exhibits reciprocation on an aqueous phase at $C_{\text{SDS-w}} = 20 \text{ mM}$, where l_x and l_y are defined in the upper of Fig.S3. l_x/l_y was the maximum when the speed of the BS droplet was zero, whereas l_x/l_y became

the minimum before the BS droplet motion reaches the maximum speed.

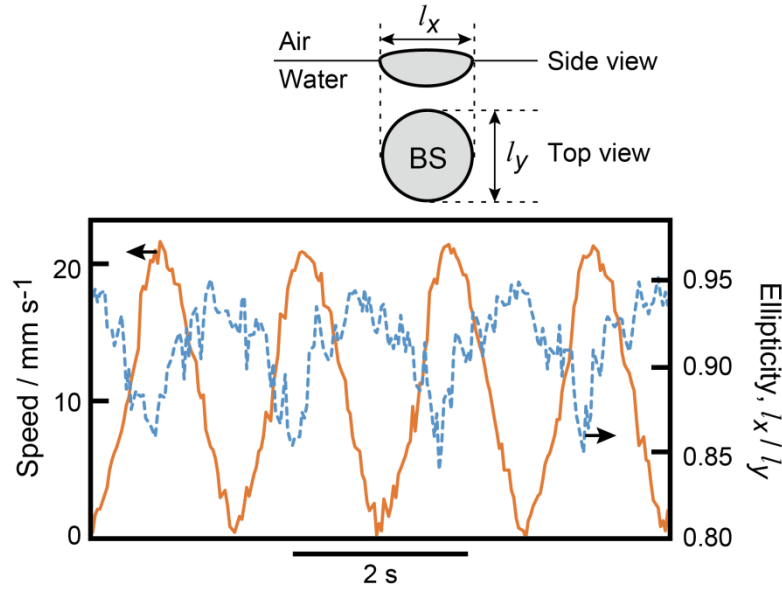


Figure S3. Simultaneous measurement of speed (solid line) and ellipticity, l_x / l_y (dotted line) for reciprocation of a BS droplet on a 20 mM SDS aqueous solution. l_x and l_y are defined schematically.

5. Contact angle, θ , estimated from eqs.1 and 2 based on the experimental results in Fig.6 and the density of SDS solutions

To confirm the validity of eqs.1 and 2, we compared the contact angle, θ , of the experimental results in Fig.4 (filled circles) with that obtained from eqs. 1 and 2 based on the experimental results in Fig.5 and the density of SDS solutions (empty circles), as shown in Figure S4. The contact angles for empty circles were similar to those for filled circles at $C_{\text{SDS-w}} < 3$ mM and at $C_{\text{SDS-w}} \geq 50$ mM, but those for filled circles were higher than those for empty circles at $3 \text{ mM} < C_{\text{SDS-w}} < 40$ mM. The range for $3 \text{ mM} < C_{\text{SDS-w}}$

< 40 mM is close to the range for reciprocation with a small amplitude. The difference of the contact angle between them may be due to the decrease in the concentration of SDS around the BS droplet since BS molecules are dissolved as the mixture of SDS and BS into the aqueous phase at this range.

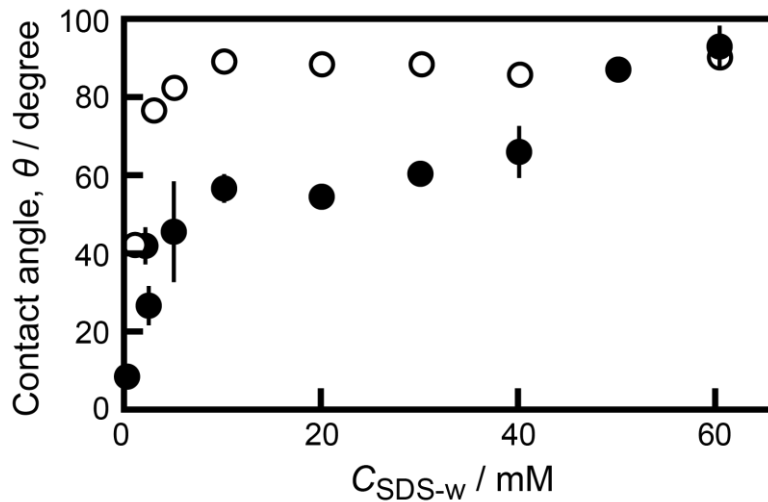


Figure S4. Contact angle, θ , of the droplet on the water phase depending on the concentration of SDS in the aqueous phase ($C_{\text{SDS-w}}$). Empty circles of the contact angle were obtained from eqs.1 and 2 based on the experimental results in Fig.5 and the density of SDS solutions. θ was measured when the droplet was inverted and the velocity of the droplet was close to zero. Filled circles correspond to the data in Figure 4.

6. Derivation of the mathematical model for BS droplet motion

We introduced the additional assumption for mathematical model. The upper phase is sufficiently thin that we can ignore its depth. Under this assumption, we can transform eq.5 into only 1-dimension model. In eq.5, s is characteristic, as the following PDE:

$$\frac{\partial s}{\partial t}(t, x, y) = d_s \Delta s. \quad (\text{S1})$$

$$\frac{1}{L_y} \int_0^{L_y} \frac{\partial s}{\partial t}(t, x, y) dy = \frac{1}{L_y} \int_0^{L_y} d_s \Delta s dy = \frac{1}{L_y} \int_0^{L_y} d_s \left(\frac{\partial^2 s}{\partial x^2} + \frac{\partial^2 s}{\partial y^2} \right) dy. \quad (\text{S2})$$

From the assumption, we consider that $\partial s / \partial t$ and $\partial^2 s / \partial x^2$ depend on y . Therefore,

from the left side of eq.S2, we obtain

$$\frac{1}{L_y} \int_0^{L_y} \frac{\partial s}{\partial t} dy = \frac{\partial s}{\partial t}, \quad (\text{S3})$$

and from the right side of eq.S2, we obtain

$$\frac{1}{L_y} \int_0^{L_y} d_s \left(\frac{\partial^2 s}{\partial x^2} + \frac{\partial^2 s}{\partial y^2} \right) dy = d_s \frac{\partial^2 s}{\partial x^2} + \frac{1}{L_y} \int_0^{L_y} d_s \frac{\partial^2 s}{\partial y^2} dy. \quad (\text{S4})$$

Then, the second term of the right side of eq.S4 is transformed as follow:

$$\frac{1}{L_y} \int_0^{L_y} d_s \frac{\partial^2 s}{\partial y^2} dy = \frac{d_s}{L_y} \left(\frac{\partial s}{\partial y}(t, x, L_y) - \frac{\partial s}{\partial y}(t, x, 0) \right). \quad (\text{S5})$$

Moreover, from the eq.8 and eq.9, the right side of eq.S4 is calculated as

$$\frac{d_s}{L_y} \left(\frac{\partial s}{\partial y}(t, x, L_y) - \frac{\partial s}{\partial y}(t, x, 0) \right) = -\frac{d_s}{L_y} \alpha (c_0 - c) u + \frac{d_s}{L_y} d_1 (s_0 - s). \quad (\text{S6})$$

Therefore, from eqs.S2-S6, we obtain

$$\frac{\partial s}{\partial t}(t, x) = d_s \frac{\partial^2 s}{\partial x^2} - \frac{d_s}{L_y} \alpha (c_0 - c) u + \frac{d_s}{L_y} d_1 (s_0 - s). \quad (\text{S7})$$

If we coordinate

$$\frac{d_s}{L_y} \alpha = k_1, \quad d_1' = \frac{d_s}{L_y} d_1 \quad (\text{S8})$$

and substitute eq.S8 for eq.S7, the following 1-dimension PDE for s is derived:

$$\frac{\partial s}{\partial t}(t, x) = d_s \frac{\partial^2 s}{\partial x^2} - k_1 (c_0 - c) u + d_1' (s_0 - s). \quad (\text{S9})$$

Similarly, we transform PDE for c in eq.5 into 1-dimension PDE and obtain the following:

$$\frac{\partial c}{\partial t} = d_c \frac{\partial^2 c}{\partial x^2} + k_1(c_0 - c)u - d_2'c. \quad (\text{S10})$$

where

$$d_2' = \frac{d_c}{L_y} d_2, \quad (\text{S11})$$

and we coordinate as

$$\frac{d_c}{L_y} \beta = k_1. \quad (\text{S12})$$

From eqs.S9 and S10, we introduce 1-dimension model for the present system as follows:

$$\left\{ \begin{array}{l} \frac{dx_c}{dt} = \frac{1}{2\mu\gamma} [\gamma(u(x_c + r), s(x_c + r)) - \gamma(u(x_c - r), s(x_c - r))] \\ \frac{\partial u}{\partial t} = d_u u_{xx} - k_u u - k_1(c_0 - c)u + F(x, x_c), \\ \frac{\partial s}{\partial t} = d_s s_{xx} - k_1(c_0 - c)u + d_1'(s_0 - s), \\ \frac{\partial c}{\partial t} = d_s c_{xx} - k_1(c_0 - c)u + d_2'c. \end{array} \right. \quad (\text{S13})$$

7. Numerical calculation of BS droplet motion

Figure S5 shows the time-course of the location and the velocity of the BS droplet with two values of s_0 , 0.02 and 0.06. The time-course of the velocities with $s_0 = 0.02$ and $s_0 = 0.06$ exhibited triangular and square like waves, respectively, similarly to the experimental data Figure 1.

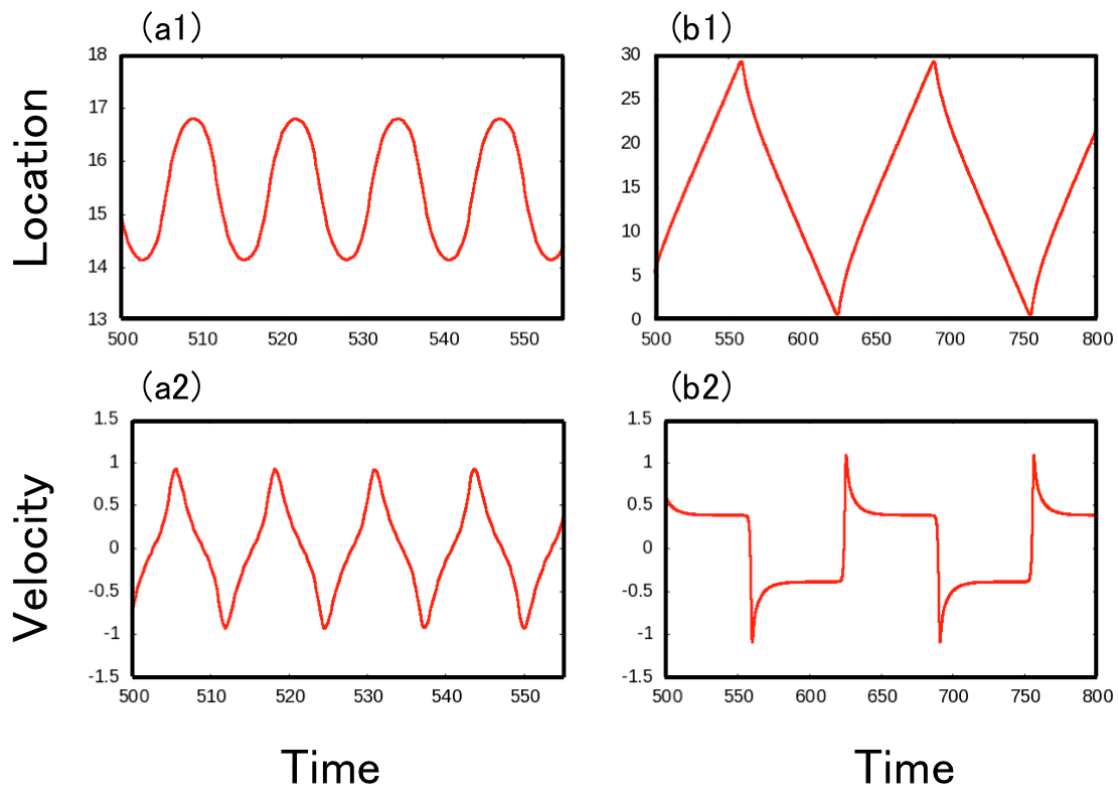


Figure S5. Time-course of (1) location of the BS droplet on the longitudinal axis of the calculating area and (2) velocity of the BS droplet at different values of s_0 ((a) $s_0 = 0.02$, (b) $s_0 = 0.06$).

8. Movies for numerical results in Figure 9

Movie S3. Movie of no motion ($s_0 = 0.005$)

Movie S4. Movie of reciprocation with a small amplitude ($s_0 = 0.02$)

Movie S5. Movie of reciprocation with a large amplitude ($s_0 = 0.06$)